Mitochondrion 30 (2016) 95–104

Contents lists available at ScienceDirect

Mitochondrion

journal homepage: www.elsevier.com/locate/mito

MitoMatters

Cardiac cytochrome c and cardiolipin depletion during anthracycline-induced chronic depression of mitochondrial function

Gonçalo C. Pereira [a,b,1], Susana P. Pereira [a,b], Ludgero C. Tavares [a,b], Filipa S. Carvalho [a,b], Silvia Magalhães-Novais [a,b], Inês A. Barbosa [a,b,2], Maria S. Santos [b], James Bjork [c,3], António J. Moreno [b], Kendall B. Wallace [c], Paulo J. Oliveira [a,*]

[a] CNC - Center for Neuroscience and Cell Biology, University of Coimbra, Biocant Park, 3060-197 Cantanhede, Portugal
[b] Department of Life Sciences, School of Sciences and Technology, University of Coimbra, 3001-401 Coimbra, Portugal
[c] Department of Biochemistry & Molecular Biology, University of Minnesota Medical School, Duluth, MN 55812, USA

ARTICLE INFO

Article history:
Received 9 April 2016
Received in revised form 5 June 2016
Accepted 12 July 2016
Available online 14 July 2016

Keywords:
Anthracycline
Cardiotoxicity
Animal model
Metabolic reserve
Cardiolipin

ABSTRACT

Aims: It is still unclear why anthracycline treatment results in a cardiac-specific myopathy. We investigated whether selective doxorubicin (DOX) cardiotoxicity involving mitochondrial degeneration is explained by different respiratory complexes reserves between tissues by comparing and contrasting treatment effects in heart vs liver and kidney. Alternatively, we have also explored if the degeneration is due to alterations of mitochondrial thresholds to incompatible states.

Methods and results: Heart, liver and kidney mitochondria were isolated from male Wistar rats weekly injected with DOX during 7 weeks. Global flux and isolated step curves were obtained for Complex I, III, IV, as well as for the adenine nucleotide translocator. We show treatment-related alterations in global flux curve for Complex III in all analyzed tissues and in Complex IV activity curve solely in heart. However, all mitochondrial threshold curves remained unchanged after treatment in the analyzed tissues. No treatment-related differences were detected on transcript or protein analysis of selected respiratory complexes subunits. However, a specific loss of cytochrome c and cardiolipin was measured in heart, but not in other organs, mitochondria from DOX-treated animals.

Conclusions: Contrary to our hypothesis, impaired mitochondrial respiration could not be explained by intrinsic differences in respiratory complexes reserves among tissues or, by alterations in mitochondrial thresholds after treatment. Instead, we propose that loss of cytochrome c and cardiolipin are responsible for the depressed mitochondrial respiration observed after chronic DOX treatment. Moreover, cardiac cytochrome c and cardiolipin depletion decreases metabolic network buffering, hindering cardiac ability to respond to increased workload, accelerating cardiac aging.

1. Introduction

Doxorubicin (DOX) is a well-known and effective anthracycline antineoplastic agent used against several human cancers (Young et al., 1981). However, one of the most limiting side-effects associated with treatment is the occurrence of a cumulative and persistent late-onset cardiotoxicity (Hequet et al., 2004; Von Hoff et al., 1979; Zhou et al., 2001). Although this cardio-specific toxicity is only present in a small fraction of patients, the associated mortality rate is very high once the diagnosis is performed (Von Hoff et al., 1979). This is not only due to the lack of sensitive methodologies to detect early stages of DOX cardiotoxicity but also the lack or absence of effective therapeutic strategies to counteract drug-induced cardiotoxicity (Singal and Iliskovic, 1998). This is partly explained by the fact that the critical mechanism behind cardiac specific DOX-induced toxicity remains to be elucidated.

Two particular aspects of sub-chronic/chronic mitochondrial cardiac alterations appear to exist in DOX-treated animal models and in human samples treated in vitro with DOX, namely loss of mitochondrial calcium-loading capacity (Montaigne et al., 2011; Santos et al., 2002; Solem et al., 1994; Wallace, 2007) and chronic decrease of mitochondrial respiration (Cini Neri et al., 1991; Ferrero et al., 1976; Santos et al., 2002; Solem et al., 1996; Solem et al., 1994; Zhou et al., 2001). Both events, of still unknown origin, appear to be cardio-selective. Hence, in the present investigation we intend to use a multi-organ approach (Pereira et al., 2012) to compare and contrast the effects of DOX-

* Corresponding author at: CNC - Center for Neuroscience and Cell Biology, UC Biotech Building, University of Coimbra, Lot 8A, Biocant Park, 3060-197 Cantanhede, Portugal.
E-mail address: pauloliv@cnc.uc.pt (P.J. Oliveira).
[1] School of Biochemistry, University of Bristol, University Walk, Bristol BS8 1TD, UK.
[2] Genetics and Molecular Medicine, King's College London, 8th Floor, Tower Wing, Guy's Hospital, Great Maze Pond, London SE1 9RT, UK.
[3] Department of Biology, University of Minnesota-Duluth, Duluth MN 55812-3025, USA.

http://dx.doi.org/10.1016/j.mito.2016.07.005
1567-7249/

treatment in heart versus liver and kidney, in order to ascertain the drug selectivity towards cardiac mitochondria.

First described by Iwamoto (Iwamoto et al., 1974), and confirmed by others, DOX toxicity underlies interference with mitochondrial Complex I. The drug is known to inhibit the respiratory complex by diverting electrons from NADH to molecular oxygen leading to DOX recycling in the process. This futile cycle is considered to be one of the major ROS production sites in DOX-induced toxicity (Davies and Doroshow, 1986). Additionally, DOX has been reported to interfere with Complex III and IV (Nicolay and de Kruijff, 1987), the phosphate carrier (Cheneval et al., 1983) and the adenine nucleotide translocator (ANT) (Oliveira and Wallace, 2006), among other mitochondrial proteins. Although most of the studies report effects in heart or cardiac-like models, some of DOX effects are shared among other tissues (Nicolay and de Kruijff, 1987; Santos et al., 2002; Yao et al., 2011). Still, DOX-induced toxicity preferentially occurs in the heart. Mazat et al. suggested that a tissue-specific phenotype may be related to the degree of enzyme inhibition and to tissue-dependent mitochondrial thresholds (Mazat et al., 1997). A mitochondrial threshold of a certain enzyme is defined as the percent inhibition before which metabolic fluxes are not or barely affected but after which a rapid decrease in flux occurs. This means that a higher threshold value for a certain mitochondrial enzyme results in a less pronounced defect in the pathway for the same degree of inhibition (Rossignol et al., 1999). Applied in the context of DOX-selective cardiotoxicity, we hypothesize that heart mitochondria are more affected by DOX treatment due to lower reserves of respiratory complex(es) compared to other tissues. An alternative hypothesis is that DOX treatment changes the threshold curve profiles to an incompatible state for high energy demands.

Both hypotheses were tested in a sub-chronic rodent model of DOX treatment previously established by Solem et al. (Solem et al., 1996) and currently in use by us (Pereira et al., 2012). This model shows cardiac mitochondrial alterations, which appear before significant ultrastructure alterations. For measuring mitochondrial thresholds, we will use the metabolic control analysis (MCA), which describes a metabolic pathway by means of a mathematical model (Moreno-Sanchez et al., 2008). Therefore, it is possible to assess how much a particular enzyme contributes to the total flux of that pathway. In our case, we measured oxidative phosphorylation (OXPHOS) with substrate transport systems, TCA enzymes, respiratory complexes, ATP synthase, ANT and phosphate carrier as enzymatic entities contributing to the global flux.

We anticipate that the results obtained will be relevant to understand the pathophysiology associated with DOX treatment in cancer patients and how that contributes to a cardiomyopathic phenotype, most likely mediated through degeneration of mitochondrial function.

2. Material and methods

2.1. Reagents

If not otherwise stated, all chemicals were of the highest purity commercially available. Detailed information is provided in the Online Supplement.

2.2. Doxorubicin solution for injection

DOX hydrochloride (Sigma-Aldrich, Barcelona, Spain), 98% chemical purity was prepared in a sterile saline solution, NaCl 0.9% (pH 3.0, HCl) and stored at 4 °C protected from light, for no longer than 5 days upon rehydration. All vials used were from the same batch.

2.3. Animal experimentation

The treatment protocol used followed the sub-chronic procedure previously established by Solem et al. (Solem et al., 1996) and adapted by us in a different strain of rats (Pereira et al., 2012). Briefly, 8 weeks old (total n = 35) male Wistar rats, Crl:WI(Han), purchased from Charles River (France), were randomly grouped in pairs and received weekly subcutaneous injection in the scruff or flank of either DOX (2 mg/Kg) or an equivalent volume of NaCl 0.9% during seven weeks, and allowed to rest one week after the last injection. More details in animal handling are provided in the Online Supplement.

2.4. Methods

A detailed explanation regarding all biochemical and molecular methods listed below can be found in the Online Supplement.

2.4.1. Mitochondrial isolation

Mitochondria from the three different tissues (heart, liver and kidney) were isolated by differential centrifugation according to the standard procedure used in our laboratory (Pereira et al., 2012). Mitochondrial protein was quantified by the biuret method (Gornall et al., 1949) using BSA as a standard.

2.4.2. Oxygen consumption

Oxygen consumption of isolated mitochondria was monitored polarographically with a Clark-type oxygen electrode connected to a suitable recorder in a 1-mL thermostated, water-jacketed, closed chamber with magnetic stirring, at 30 °C. Details regarding mitochondrial energization, ADP phosphorylation and inhibitor titrations are found in the Online Supplement.

2.4.3. Enzyme activities

All assays follow microplate adaptations of previous well-established standard methods for the evaluation of respiratory enzyme activities (Birch-Machin and Turnbull, 2001; Long et al., 2009; Luo et al., 2008; Spinazzi et al., 2011). Enzyme activity was followed by the decrease in DCPIP absorbance upon addition of NADH for Complex I; increase in absorbance of oxidized cytochrome c upon addition of decylubiquinol for Complex III; and decrease in absorbance of reduced cytochrome c for Complex IV. Hexokinase activity in isolated mitochondrial fractions was assessed using a hexokinase assay linked to $NADP^+$ reduction.

2.4.4. Lipids extraction and cardiolipin quantification

Total lipids of isolated cardiac mitochondrial fractions were extracted by the Bligh and Dyer method (Bligh and Dyer, 1959) and quantified by the phosphorus assay (Bartlett and Lewis, 1970). Total lipid extracts were separated into different classes by thin layer chromatography and cardiolipin was then quantified by the above mentioned methodology.

2.4.5. Western blot

Proteins in RNAlater-conserved frozen tissues were extracted in RIPA buffer, supplemented with protease inhibitors cocktail, and then diluted in Laemmli buffer after protein quantification by the BCA method. Afterwards, proteins were separated by an SDS-PAGE and electrotransferred to a PVDF membrane. Primary antibodies against the protein of interest were used and are listed in Table S1 of the Online Supplement. For protein detection an enhanced chemi-fluorescence (ECF) kit was used and the membrane imaged by using the Versa Doc imaging system (Bio-Rad, Barcelona, Spain). Density of different bands was calculated with Quantity One Software (Bio-Rad).

2.4.6. Quantitative real-time PCR

Total tissue mRNA was extracted using RNeasy Mini Kit (Qiagen Inc., Valencia, CA, USA). RNA transcripts levels were quantified by real-time reverse transcriptase - (RT) polymerase chain reaction (PCR) involving two separate steps: first, cDNA was synthesized from extracted RNA; secondly, real-time PCR FastStart SYBR Green I Kit (Roche Diagnostics, Indianapolis, IN, USA). Samples were quantified using a serial dilution of a well characterized DNA standard and 18S ribosomal RNA was used to normalize gene expression. A fully detailed methodology is provided in the Online Supplement.

2.4.7. Statistical analysis

Briefly, statistical significance between means of saline and DOX groups was determined using two-tailed Student's *t*-test. In the specific case when seeking to ascertain whether changes between saline and DOX group in the heart are actually different from changes in other tissues, regardless of the inter-tissue baseline (i.e. for mRNA and protein

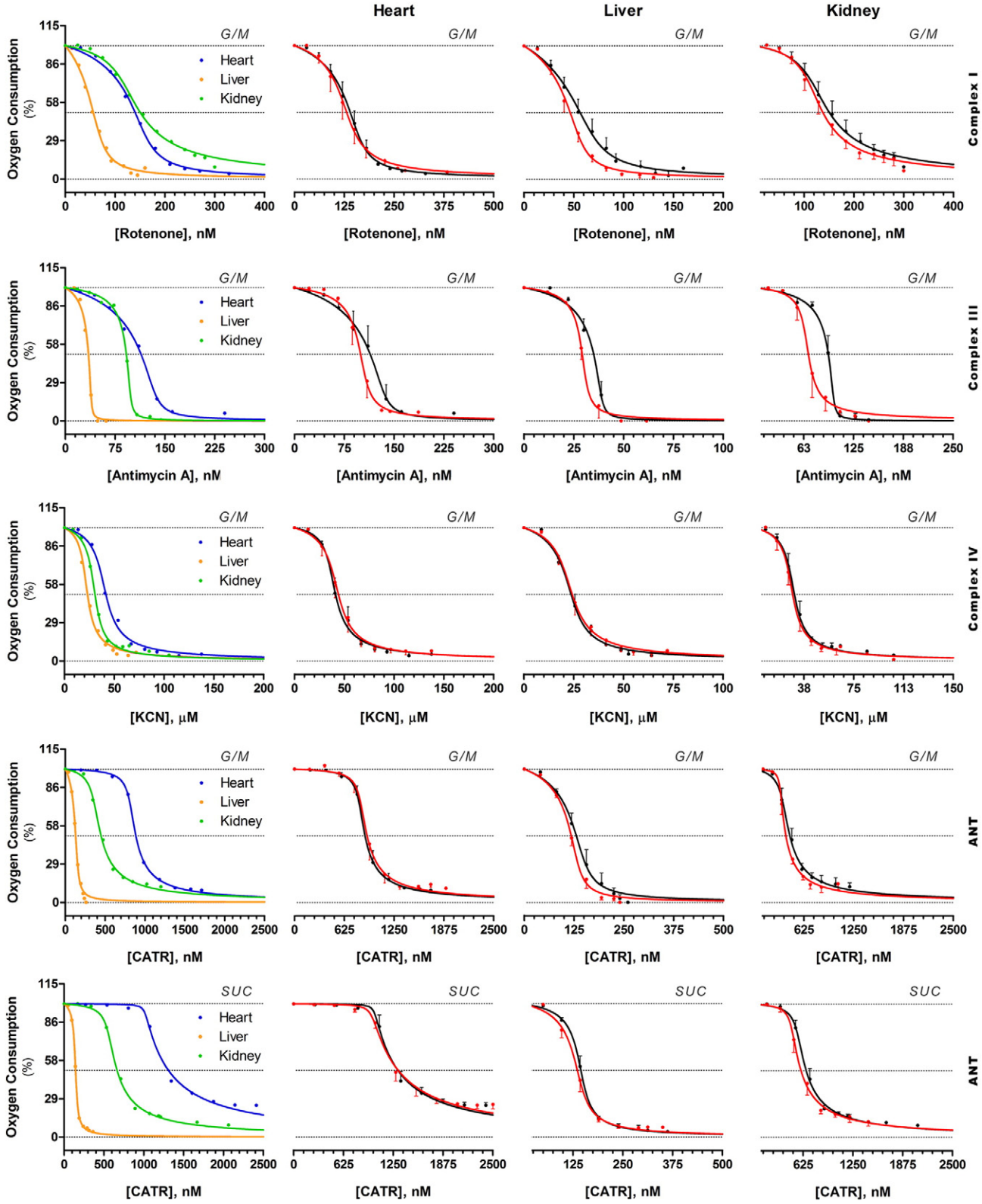

Fig. 1. Effect of sub-chronic DOX treatment on dose-response curves of mitochondrial oxygen consumption. Oxygen consumption rates were evaluated and processed as described in Material and Methods. Dots represents the mean of each titration points (n = 4–7) with SE (black pointing upwards - saline; red pointing down - DOX). Error bars are smaller than symbols when not visible and are absent in the first column of graphs where only saline group is represented. Abbreviations: G/M - glutamate-malate; SUC - succinate; KCN - Potassium cyanide; CATR - carboxyatractyloside.

content) data were analyzed by a two-way ANOVA with planned contrasts against the interaction between treatment and tissue so that significant relative changes (fold-change) are dependent on tissue. p-Values were thereafter adjusted for multiplicity using Šídák post-hoc test. Statistical analyses were performed using Graph Pad Prism version 5.0 (GraphPad Software, Inc., San Diego, CA, USA), with the exception of the two-way ANOVA which was performed using JMP-SAS version 9.03 (SAS Campus Drive, Cary, NC, USA). Non-linear regressions and simulations were performed using Graph Pad Prism. Further details are given in the Online Supplement. In order to ascertain whether traces (plots) were statistically different between tissues or treatment, the extra sum-of-squares followed by an F test ($p < 0.05$) was used to determine if a single curve adequately fitted all the data points in the analyzed groups. In the text, data is expressed as percentage of the difference of means plus its standard error.

3. Results

3.1. Mitochondrial threshold in all tissues remains constant after DOX treatment

We have previously characterized a sub-chronic rodent model of DOX-induced toxicity and reported that alterations in mitochondrial physiology occur in the absence of changes in cardiac biochemical markers or cardiac structure/function assessed by echocardiogram (Pereira et al., 2012), representing a sub-clinical marker of DOX cardiotoxicity.

For the present investigation, our analysis focused on three respiratory complexes (I, III and IV) and in the ANT using the same sub-chronic animal model. Mitochondrial threshold curves originated from the titration curves of the global flux and isolated step. The obtained data for each step is reported independently in the following sections.

3.1.1. Global step - titration curves of oxygen consumption

Global flux was evaluated through oxygen consumption in the presence of excess ADP, i.e. state 3 respiration rate, sustained by Complex I-linked substrates for the analysis of Complex I, III and IV. For the ANT, a protocol similar to what was previously established in our group was used (Oliveira and Wallace, 2006). Table S3 shows the maximal state 3 respiration rates for each tissue and treatment group and were found to be consistently lower in cardiac mitochondria from DOX-treated rats, as previously reported (Pereira et al., 2012).

3.1.1.1. Inter-tissue comparisons. The first column of Fig. 1 shows the titration curves profile of OXPHOS inhibitors for the different tissues. The traces were significantly distinct ($p < 0.05$, determined by the extra sum-of-squares followed by an F test) regardless of the tissue of origin or respiratory complex analyzed. Two parameters were obtained from the curve-fitting model and were used to characterize the different mitochondrial preparations (Table 1). Overall, the control coefficients (C^I) for the respiratory complexes were variable among tissues. Although one has used a curve fitting procedure (Gellerich et al., 1990) instead of the "bottom up" approach (Groen et al., 1982) to determine the flux control coefficients the obtained values were still scattered. This in part explains the lack of statistical significance observed when comparing C^I between tissues ($F_{2,20} = 3.48$, $p = 0.050$ for Complex I; $F_{2,18} = 2.99$, $p = 0.076$ for Complex III; and, $F_{2,20} = 0.630$, $p = 0.543$ for Complex IV). Regarding the ANT, its C^I value was several fold times higher in liver compared to heart and kidney under Complex I or II-sustained respiration.

In the present study, respiratory complexes in cardiac mitochondria contributed to 49.0 ± 12.1% of the global flux with its highest C^I shared between Complex I and III (~0.20). The remaining mitochondrial preparations presented two opposite extremes. Liver mitochondria showed high dependency (79.1 ± 18.2%) on the respiratory complexes due to their C^I being consistently >0.10, except for Complex III. Conversely, C^I in kidney mitochondria was consistently lower than 0.09 which explains the low observed contribution for the global flux (21.8 ± 6.4%).

The total apparent/theoretical enzyme content (E^0) of each OXPHOS complex was also different between tissues (Table 1). Cardiac mitochondria consistently presented the highest E^0 of any of the evaluated respiratory complexes while hepatic mitochondria presented the lowest. Among the evaluated enzymatic complexes, Complex IV was the protein with highest E^0 regardless the tissues of origin while the E^0 for Complex III was systematically lower.

Overall, cardiac mitochondria present a high content of respiratory complexes although their contribution to OXPHOS is moderate.

3.1.1.2. DOX treatment-dependent effects. In vivo sub-chronic treatment with DOX induced a significant left-shift on the titration curves of Complex III (Fig. 1). However, the effect does not seem to be cardio-specific as liver and kidney mitochondria also presented the same alteration ($p < 0.05$). Interestingly, this change was followed by a significant decrease in E^0 for this OXPHOS step in cardiac and kidney mitochondria (25.4 ± 10.8% and 45.1 ± 5.1%, respectively; Table 1) but not in liver.

Table 1
Best-fit parameters from the fitting of global flux curves.

		Heart				Liver				Kidney			
	Treat.	C^I		E^0		C^I		E^0		C^I		E^0	
		Mean	SE	Mean	SE	Mean	SE	Mean	SE	Mean	SE	Mean	SE
Complex I	Saline	0.194	0.090	155.4[a]	20.3	0.431	0.145	80.4	9.6	0.066	0.033	120.6	15.3
	DOX	0.120	0.063	128.9	18.3	0.273	0.126	53.7	8.6	0.090	0.046	122.0	16.0
Complex III	Saline	0.203	0.073	136.8[a, c]	10.1	0.047	0.033	32.6[b]	2.7	0.068	0.034	99.3	4.3
	DOX	0.072	0.038	102.1[*]	10.8	0.062	0.033	30.2	1.6	0.004	0.007	54.5[***]	2.8
Complex IV	Saline	0.075	0.042	38.7[a]	4.1	0.134	0.053	23.9	2.6	0.069	0.040	29.2	0.1
	DOX	0.074	0.044	41.1	4.5	0.106	0.042	23.1	2.5	0.070	0.040	27.9	2.9
ANT (G/M)	Saline	0.018	0.016	827.7[a, c]	56.2	0.178[a, b]	0.070	150.2[b]	14.6	0.015	0.015	335.2	23.8
	DOX	0.018	0.012	844.9	49.8	0.176	0.078	131.8	13.6	0.022	0.023	343.9	27.8
∑	Saline	0.490	0.121	n.a.	n.a.	0.791	0.182	n.a.	n.a.	0.218	0.064	n.a.	n.a.
	DOX	0.283	0.086	n.a.	n.a.	0.617	0.165	n.a.	n.a.	0.187	0.066	n.a.	n.a.
ANT (SUC)	Saline	0.003	0.007	1020.0[a, c]	41.5	0.083[a]	0.029	147.7[b]	7.4	0.021	0.017	561.6	47.3
	DOX	0.003	0.006	976.9	41.8	0.090	0.028	140.2	7.0	0.021	0.015	495.2	28.8

Data refers to best-fit values obtained from the curve-fitting on Fig. 2 where C^I is unitless and E^0 is in the same units as its correspondent curve abscissa in Fig. 2. ∑ represents the sum of control coefficients of each respiratory complex except the ANT in the presence of succinate. Inter-tissue comparisons were as follows: [a], $p < 0.05$ heart vs. liver. [b], $p < 0.05$ liver vs. kidney. [c], $p < 0.05$ kidney vs. heart. Within the same respiratory complex group, as evaluated by a one-way ANOVA followed by pair-wise comparisons through Bonferroni's post-hoc analysis. Intra-tissue comparisons were evaluated by an unpaired Student's *t*-test with Welch's correction whenever data was not homoscedastic.
Abbreviations: Treat. - treatment; SE - standard error; C^I - control coefficient; E^0 - enzyme concentration in the absence of inhibitor; G/M - glutamate/malate; SUC - succinate; ANT - adenine nucleotide translocase; n.a. - not applicable.
[*] $p < 0.05$ vs. saline group.
[***] $p < 0.001$ vs. saline group.

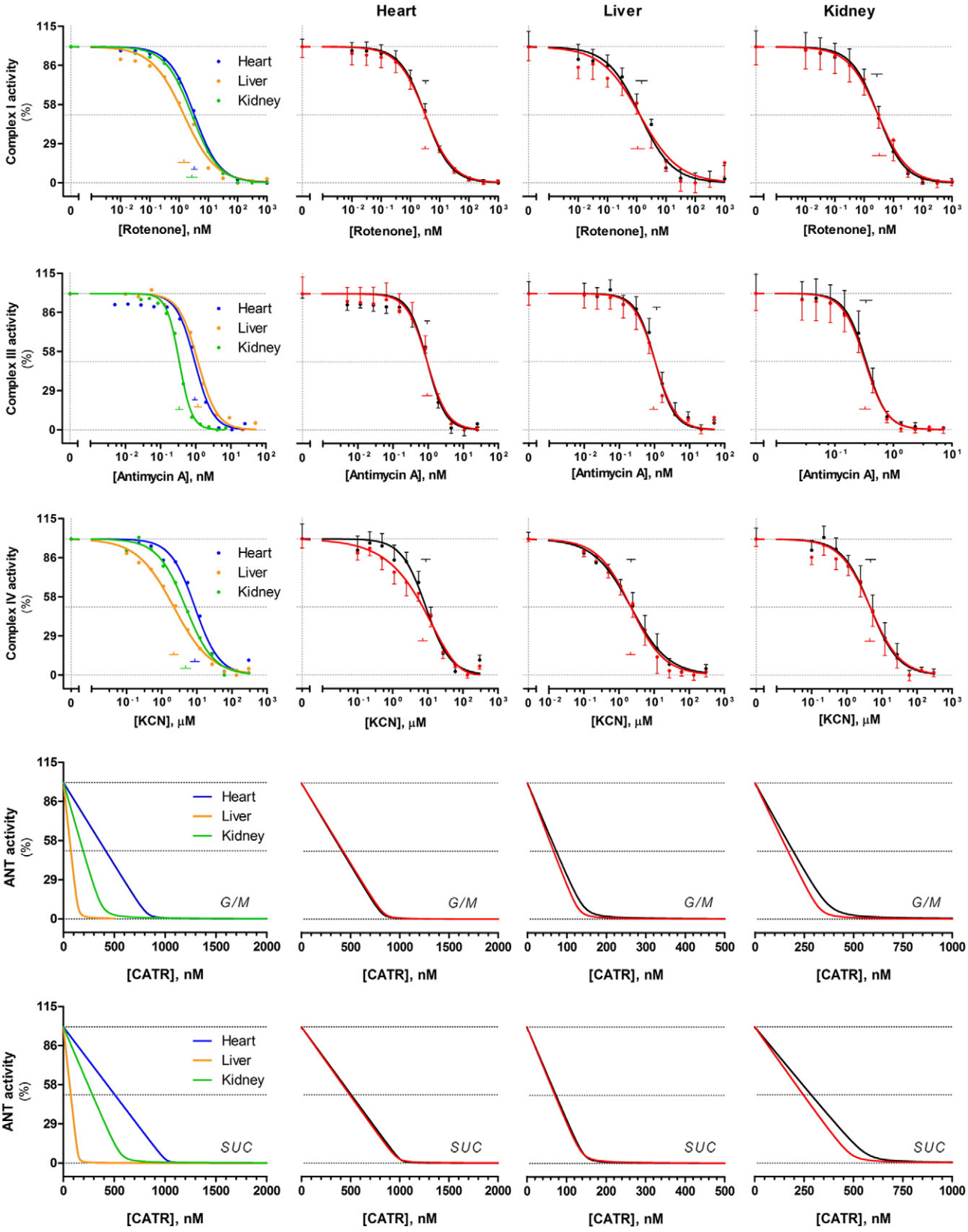

Fig. 2. Effect of sub-chronic DOX treatment on dose-response curves profile of OXPHOS complexes activity. Dots represents the mean of each titration points (n = 5) with SE (black pointing upwards - saline; red pointing down - DOX). Error bars are smaller than symbols when not visible and are absent in the first column of graphs where only saline group is represented. Also depicted are IC_{50}: vertical arm of the small T represent mean value and horizontal arm the respective 95% CI. Abbreviations: G/M – glutamate/malate; SUC - succinate; KCN - Potassium cyanide; CATR - carboxyatractyloside.

No alteration in C^I for Complex III was observed regardless of the tissue analyzed.

Regarding the remaining respiratory complexes, DOX treatment induced minor alterations on the titration curves of Complex I, IV and ANT in heart (Fig. 2, $p > 0.05$). Therefore, no differences were found in C^I and E^0 values between both groups (Table 1). However, DOX treatment also induced a left-shift in the titrations curves of Complex I in liver ($p < 0.001$) and of the ANT with Complex II-sustained respiration in kidney ($p = 0.046$). Still, no alterations in C^I or E^0 were observed in any of the organs. The remaining curves as well as their respective C^I and E^0 values were similar between treatment groups both in liver and kidney mitochondria.

Despite the general decrease in the sum of control coefficients observed in all mitochondrial preparations after DOX treatment no statistical significance was obtained (Table 1). Also, there was no treatment-related effect regarding ANT mobilization upon Complex II-sustained respiration in any of the mitochondrial preparations.

3.1.2. Isolated step - OXPHOS complexes activity dose-response curves

The second step in the evaluation of mitochondrial thresholds is the evaluation of isolated steps. In the present case, the isolated step represents the maximal enzymatic activity. Table 2 summarizes the maximal activity of selected OXPHOS enzymes for each tissue and treatment group. It is apparent that all tissues present a V_{max} different from each other but similar between treatment groups with the following exceptions: Complex III activity in liver mitochondria from DOX-treated rats was significantly lower when compared to control while Complex IV activity in heart and kidney from DOX-treated rats was significantly higher compared to their control counterparts.

Despite the above mentioned effects on V_{max} the inhibition curves were similar between treatment group (Fig. 2) with the exception of Complex IV in heart mitochondria, where a five parameter logistic (5PL) curve-fitting was preferred over the four parameter logistic (4PL) used for the control group. Nevertheless, IC_{50} for all OXPHOS respiratory complexes remained unchanged after DOX treatment (Table S4) suggesting similar protein level between treatment groups.

3.1.3. Mitochondrial thresholds curves

The last step in the evaluation of mitochondrial thresholds for OXPHOS enzymes is the generation of threshold curves emerging from the titration curves of the global flux (Fig. 1) and isolated step (Fig. 2). Therefore, it represents state 3 respiration rate as a function of OXPHOS enzyme inhibition. Fig. 3 shows that threshold curves for the OXPHOS enzymes evaluated in this work are mainly Type I. Type I curves are characterized by a well-defined initial plateau which remains constant until a certain value of inhibition where a sharp decline occurs. Conversely, in Type II curves the initial plateau is not evident and therefore no sudden change in flux is observed (Rossignol et al., 1999). Consequently, Type I curves are characterized by high thresholds which is in agreement with that found in the present investigation (Table 3).

Analysis of the curves presented in Fig. 3 shows that sub-chronic treatment with DOX did not alter significantly the profile of the threshold curves of OXPHOS respiratory complexes for the three tissues analyzed in the present work. Consequently, the threshold values for the different complexes remained unchanged (Table 3). Regarding ANT curves, only minor differences can be detected. Despite the upper right drag of the curve, the threshold value only increased about 4% for kidney mitochondria from DOX-treated rats.

Despite the above mentioned alterations, the fitness of DOX-treated mitochondria to phosphorylate exogenous-added ADP under basal conditions (i.e. no inhibitors added) remains unaffected, with exception of kidney mitochondria (Fig. S1). The energy charge in mitochondria from heart and liver was similar between treatment groups regardless of the tissue or respiratory substrate in study, suggesting that the depressed electron transfer may only be observed in vivo after accumulation of defects.

3.2. Transcript and protein level of OXPHOS complex subunits remain constant after DOX treatment

To further investigate the alterations in metabolic fluxes, we evaluated transcript content for selected OXPHOS respiratory complexes subunits. Fig. S2 summarizes Table S5 as a heat-map representation of the transcript levels of selected OXPHOS complexes subunits evaluated by qRT-PCR. Despite the apparent alterations depicted in Fig. S2 the statistical test applied did not retrieve significant results (Table S5).

Although no statistically significant alterations in mRNA were found, protein content of some OXPHOS complexes subunits was analyzed by Western blotting. At least one protein subunit from each complex was analyzed through this methodology (Table S6). As can be seen in the heat-map representation in Fig. S3 taken from the data in Table S6, all protein levels remained similar to control after sub-chronic treatment with DOX regardless of the respiratory complex or tissue being analyzed.

3.3. Cardio-selective loss of mitochondrial cytochrome c and cardiolipin

The absence of alterations on the transcript and protein levels of the OXPHOS complexes in study, the similar IC_{50} of respiratory complexes after DOX treatment but low state 3 respiration and E^0 for Complex III suggests that OXPHOS network buffering capacity might be compromised after DOX sub-chronic treatment. Due to the specific effect on E^0 for Complex III and the left-shift on its global-flux curve we then focused our analysis on cytochrome c in the different mitochondrial preparations. Fig. 4 shows that mRNA and protein level of cytochrome c in total heart extracts were not different comparing saline and DOX-treated animals (Fig. 4, panel A and B). Likewise, no treatment-related alteration was observed in liver or kidney. However, when cardiac isolated mitochondrial fractions were analyzed, the cytochrome c content was $13.3 \pm 5.2\%$ lower in DOX-treated group (Fig. 4, panel B). This was a cardiac-specific alteration since liver and kidney mitochondria from DOX-treated animals had identical levels compared to their saline counterparts.

Cardiolipin is an inner mitochondrial membrane (IMM) anionic phospholipid that provides an anchor to cytochrome c by means of electrostatic and hydrophobic interactions, being also involved in its release under apoptotic stimuli (Ott et al., 2002). In our model, we found that cardiolipin content is decreased by $21.9 \pm 8.4\%$ in cardiac mitochondria after sub-chronic treatment with DOX (Fig. 4C), possibly resulting in higher mobility of cytochrome c in the intermembrane space. No alteration was observed in liver or kidney mitochondria.

Table 2
Effect of sub-chronic DOX treatment on mitochondrial respiratory complexes maximal activity.

Complex	Treat.	Heart		Liver		Kidney	
		Mean	SE	Mean	SE	Mean	SE
		n = 5		n = 5		n = 5	
Complex I[a]	Saline	260.1	9.8	19.7	2.0	158.5	15.0
	DOX	248.5	16.4	16.8	0.9	161.9	16.2
Complex III[b]	Saline	207.5	2.8	19.8	1.7	60.6	9.0
	DOX	250.1	31.0	16.3*	0.8	63.7	7.5
Complex IV[c]	Saline	1789.0	160.3	534.9	22.8	835.8	59.1
	DOX	2311.0*	138.3	538.9	22.1	964.6*	38.9

Tabulated values represent absolute values of the maximal specific activity of each respiratory complex which was calculated as the difference between the activity in the absence of inhibitor and the activity in the presence of the highest concentration of inhibitor.
Abbreviations: Treat. - treatment.

* $p < 0.05$ vs. saline group within the same tissue and respiratory complex group, as evaluated by a paired Student's *t*-test.

[a] Activity expressed as nmol DCPIP min/mg protein.

[b] Activity expressed as (increase) nmol cyt c_{red}/min/mg protein.

[c] Activity expressed as (decrease) nmol cyt c_{red}/min/mg protein.

In these circumstances, an increased permeability of the outer mitochondrial membrane could explain the redistribution of cytochrome c from the mitochondria to the cytosol. Bax and hexokinase II (HK2) are two important players in outer mitochondrial membrane permeabilization (Kroemer et al., 2007). Unfortunately, when cardiac mitochondrial fractions were analyzed by Western blot for evaluation of

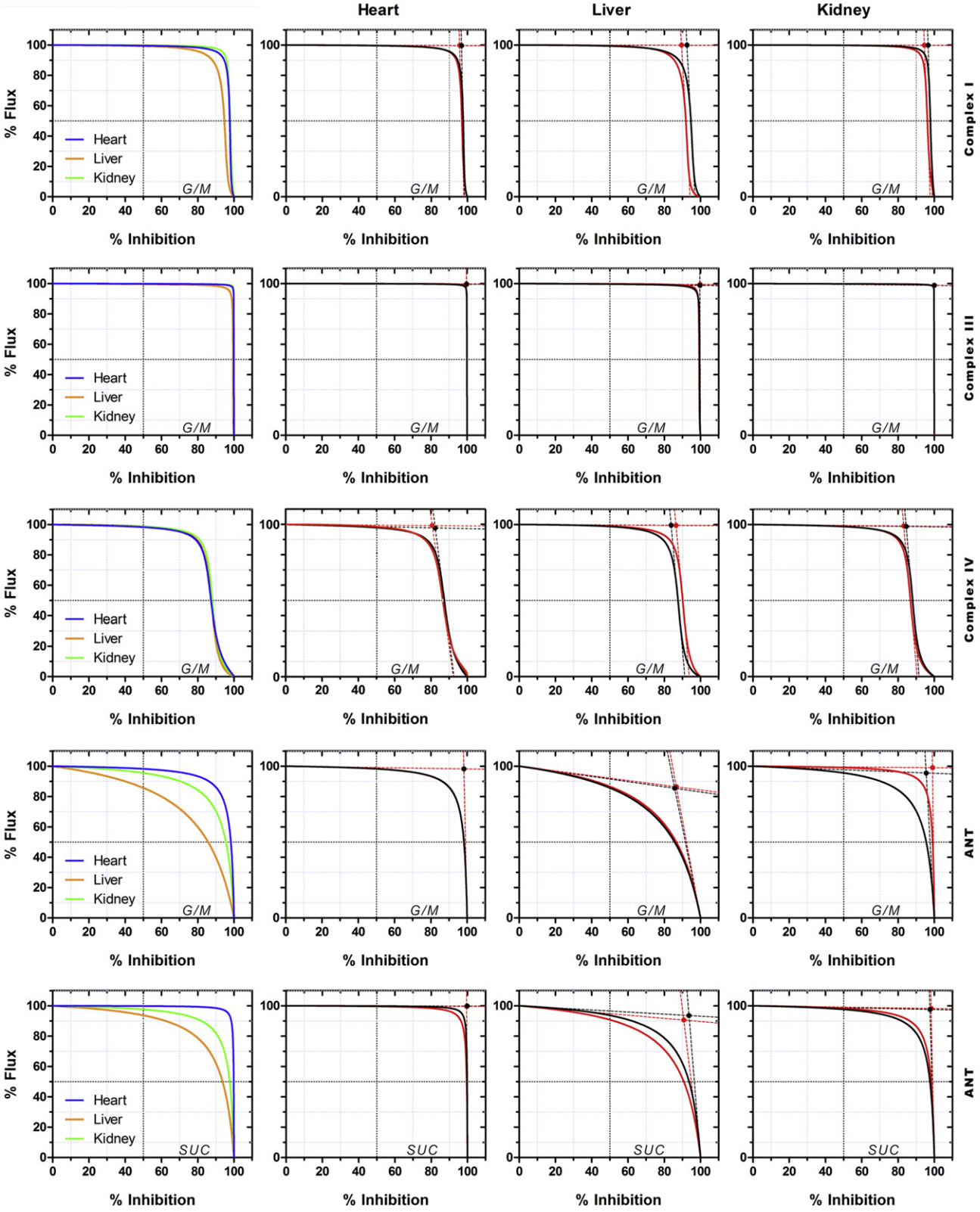

Fig. 3. Effect of sub-chronic DOX treatment on the profile of mitochondrial thresholds curves for OXPHOS complexes. Curves were simulated as described in Material and Methods using the parameters obtained from the fitting of curves shown in Figs. 2 and 3. Dashed lines represent linear regressions at the beginning (1% inhibition) and at the end (inflection point) of the curve, and were used to determine the threshold value which is represented by the full circle. Absolute values of the thresholds are presented in Table 3. Black – saline, Red – DOX. Abbreviations: G/M - glutamate-malate; SUC - succinate.

these two proteins, the obtained signal was extremely low and not suitable for quantification. In cardiac tissue and after an ischemic insult, total HK activity correlates with the amount of HK2 that remains bound to mitochondria (Pasdois et al., 2013). Thus, as an alternative, we measured the total HK activity in the cardiac mitochondrial fractions in order to infer the amount of protein present in the sample. Total HK activity was higher in DOX-treated group by 84.3 ± 23.5% when compared to control (Fig. S4).

Although the homogenization procedure during mitochondria isolation rather than DOX-treatment itself could affect the integrity of mitochondrial membranes promoting cytochrome c release, both the isolation yield (Table S7) and cytochrome c oxidase subunit I and IV levels (Fig. S3) were similar between treatment groups. Moreover, electron micrographs show that heart mitochondria from DOX-treated animals do not differ significantly from the control group (Fig. S5). Hence, cardiac cytochrome c and cardiolipin depletion cannot be attributed to selection of a sub-mitochondrial population or to damage to the organelle during the isolation procedure.

4. Discussion

In the present study, through differential analysis of tissues from DOX-treated animals, we were able to detect cardio-specific mitochondrial alterations, namely cardiolipin and cytochrome c depletion that contribute to the worsening of DOX-induced toxicity. The animal model used was initially developed by Solem and colleagues (Solem et al., 1996) and is based on lower dosage administered over a few weeks period. Animals develop cardiac structural alterations similar to those observed in DOX-induced cardiotoxicity in patients (Singal and Iliskovic, 1998). More recently, we have applied the same sub-chronic treatment protocol to a different rat strain (Wistar) and observed that it elicits persistent mitochondrial alterations that are specific to cardiac tissue and are present in the absence of structural or functional alterations in the heart (Pereira et al., 2012). In the current investigation by contrasting the effects of treatment on heart versus liver and kidney, we suggest that loss of cardiolipin and cytochrome c redistribution may contribute to DOX tissue specificity and development of cardiotoxicity through impaired mitochondrial function. Moulin et al. has also demonstrated that cardiolipin loss is sex-specific, occurring preferentially in male, using Wistar rats and a similar treatment protocol (Moulin et al., 2015). Interestingly, animals presented both depressed cardiac function and signs of cardiomyopathy. Although the findings of our work are consistent with a cardio-selective toxicity it does not prove cause and effect.

Our starting hypothesis was based on DOX effects on respiratory complexes and mitochondrial carriers (Cheneval et al., 1983; Davies and Doroshow, 1986; Nicolay and de Kruijff, 1987; Oliveira and Wallace, 2006; Yao et al., 2011). We had anticipated that OXPHOS enzymatic reserves were lower in the heart or, alternatively, that OXPHOS in heart mitochondria was dependent in one particular respiratory complex, more so than liver or kidney. However, following MCA theory (Moreno-Sanchez et al., 2008) we demonstrated that OXPHOS is not controlled by a single enzyme or limiting step. In fact, C^I distribution showed that heart and liver are primarily controlled by the respiratory chain while kidney is controlled more at phosphorylation level, as previously reported (Moreno-Sanchez et al., 2008; Rossignol et al., 2000). Moreover, mitochondrial thresholds for the different OXPHOS enzymes were consistently >80%. Altogether, results demonstrate that DOX-induced cardiac specific toxicity cannot be solely attributed to intrinsic differences between tissues on OXPHOS control or enzymatic reserves.

Instead, we observed a shift towards lower inhibition of Complex III while monitoring mitochondrial respiration across all tissues. This was translated in a lower E^0 in heart and kidney. Still, individual enzymatic analysis of Complex III revealed treatment-related differences only in liver. The lack of effect on the maximal enzyme activity in heart and kidney suggests that the effect was not directly on Complex III protein but rather in other(s) proteins of the network. This was the rationale for the evaluation of cytochrome c levels. Similarly, the higher Complex IV activity reported for the isolated-step may not be observed while evaluating the global flux because its contribution into the metabolic network is small. In conclusion, data obtained in Table 1 reflect effects over a wide range of proteins while the data in Table 2 is restricted to the respiratory complex itself.

The asymmetry, i.e. transition from a 4PL to a 5PL curve fitting, observed for Complex IV activity curve in cardiac mitochondria after DOX treatment was not translated into alterations in the threshold curve of the respiratory complex. This is due to the combination of distinct aspects of heart mitochondria: 1) its low OXPHOS control coefficient (C^I) means that only effects observed at high inhibitor concentrations will affect the threshold curve, i.e. long plateau of threshold curve; 2) the treatment-induced asymmetry occurs on the top part of the curve and thus its effect is reduced on the threshold curve due to its long plateau. In conclusion, DOX treatment does not change the threshold curve profiles to an incompatible state for high-energy demands.

Unfortunately, one cannot explain the reason for cardiolipin loss; however, the increased oxidative stress experienced in our animal model (Pereira et al., 2012) can lead to cardiolipin oxidation and thus its removal. Alternatively, the interaction of DOX molecule with cardiolipin (Parker et al., 2001) can also facilitate its oxidation.

Another limitation of the present work is the fact that we could not explain the mechanism underlying cytochrome c release. The extremely low levels of two possible protein candidates, Bax and HK2, hindered any conclusion. It could mean that only a small amount of Bax translocated to mitochondria or that in general proteins attached to OMM were lost during the isolation protocol. That could additionally explain why our total HK activity in mitochondrial fractions is just one third of that reported in the literature (Pasdois et al., 2013). Nevertheless, once in cytoplasm, free cytochrome c can interact with Apaf-1 and pro-caspase 9 activating the latter and consequently lead to activation of caspase 3, as we have previously reported in heart (Machado et al., 2010).

Alternatively, the present data could also be analyzed in the light of the aging theory and through comparison to a previous report where it was demonstrated that the failing heart in aging results from the loss of respiratory supercomplexes (Gomez et al., 2009). Gómez et al. suggested that destabilization of inter-fibrillar mitochondrial string supercomplexes is the responsible for the decline in mitochondrial function during aging (Gomez et al., 2009). Moreover, the authors pointed the possible role of Complex IV in the underlying mechanism as it is the only respiratory complex present in all supercomplexes. Additionally, loss or mutations in certain subunits of Complex IV are

Table 3
Threshold values of the different OXPHOS complexes.

Complex	Treat.	Heart	Liver	Kidney
		Mean	Mean	Mean
		%		
Complex I	Saline	96.8	92.5	96.6
	DOX	95.7	89.6	94.6
Complex III	Saline	99.7	99.6	100.0
	DOX	99.6	99.8	100.0
Complex IV	Saline	82.4	83.8	84.5
	DOX	82.9	86.5	83.2
ANT (GM)	Saline	98.2	85.8	95.6
	DOX	98.3	86.7	99.1
ANT (SUC)	Saline	99.8	93.7	97.6
	DOX	99.6	90.8	98.3

Threshold value was defined as the abscissa of the intersection point between the two tangents obtained from Fig. 4.
Abbreviations: Treat. - treatment; G/M - glutamate-malate; SUC – succinate; ANT – adenine nucleotide translocator.
There were no statistically significant differences across treatment or tissue.

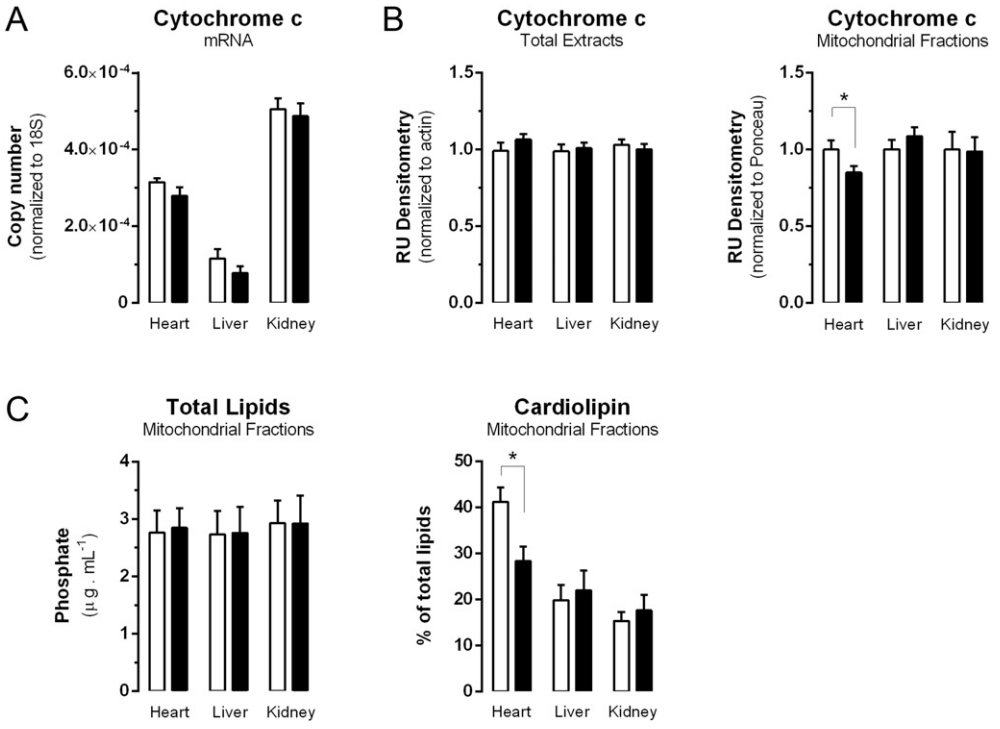

Fig. 4. Effect of sub-chronic DOX treatment on cytochrome c and cardiolipin content. A – total mRNA of cytochrome c in whole-tissue extracts (n = 8); B – Total cytochrome c protein levels in the different tissues (left, n = 8) as well as cytochrome c content in isolated mitochondrial fractions (right, n = 6). C – total lipids and cardiolipin content in isolated mitochondrial fractions (n = 6). Bars represent means of treatment groups (saline in white bars; DOX in black bars) with SE. Differences between treatment groups means were evaluated by Student's *t*-test (matched pairs for isolated mitochondria samples). *, $p < 0.05$ vs. saline group.

associated with destabilization of supercomplexes (Gomez et al., 2009). Since DOX treatment decreased cardiolipin content in heart mitochondria, a crucial component in the biogenesis and stabilization of supercomplexes as well as for the activity of Complex IV, it may be rationale to consider that another possible mechanism is alteration of the stability of mitochondrial supercomplexes.

5. Conclusion

Contrary to our working hypothesis, there was no apparent difference in OXPHOS respiratory threshold between mitochondria isolated from heart, liver or kidney tissues. Therefore, one cannot imply that the heart is more sensitive due to higher dependence on one particular complex. In fact, the initial hypothesis on which this work was based was not supported by the results of this investigation. However, a cardio-specific effect was detected for cytochrome c redistribution and lower cardiolipin content. This may well be a reasonable explanation for the decrease in oxygen consumption during state 3, despite no alterations in the expression and content of OXPHOS components, emphasizing the importance of cardiolipin and cytochrome c redistribution in DOX-induced specific cardiotoxicity. Nevertheless, due to this alteration in electron transfer, cardiac mitochondria from DOX-treated rats may not have the fitness and elasticity to adapt to higher energy demands thus contributing to an accelerated cardiac degenerative phenotype.

Disclosures

The agencies had no role in the manuscript contents or decision to publish. None of the authors has disclosed any conflict of interest.

Source of funding

This work was supported by FEDER funds through the Operational Programme Competitiveness Factors - COMPETE and national funds by FCT - Foundation for Science and Technology under the project PTDC/DTP-FTO/1180/2012 and strategic project UID/NEU/04539/2013. The work was also supported by QREN project #4832 “Stemcell based platforms for Regenerative and Therapeutic Medicine”, with reference “CENTRO-07-ST24-FEDER-002008”.

The FCT also supported doctoral fellowships [SFRH/BD/36938/2007 to G.P., SFRH/BD/64247/2009 to S.P., SFRH/BD/66600/2009 to L.T., SFRH/BD/64694/2009 to F.C. and SFRH/BD/48157/2008 to I.B.].

Appendix A. Supplementary data

Supplementary data to this article can be found online at http://dx.doi.org/10.1016/j.mito.2016.07.005.

References

Bartlett, E.M., Lewis, D.H., 1970. Spectrophotometric determination of phosphate esters in the presence and absence of orthophosphate. Anal. Biochem. 36, 159–167.
Birch-Machin, M.A., Turnbull, D.M., 2001. Assaying mitochondrial respiratory complex activity in mitochondria isolated from human cells and tissues. Methods Cell Biol. 65, 97–117.
Bligh, E.G., Dyer, W.J., 1959. A rapid method of total lipid extraction and purification. Can. J. Biochem. Physiol. 37, 911–917.
Cheneval, D., Muller, M., Carafoli, E., 1983. The mitochondrial phosphate carrier reconstituted in liposomes is inhibited by doxorubicin. FEBS Lett. 159, 123–126.
Cini Neri, G., Neri, B., Bandinelli, M., Del Tacca, M., Danesi, R., Riccardi, R., 1991. Anthracycline cardiotoxicity: in vivo and in vitro effects on biochemical parameters and heart ultrastructure of the rat. Oncology 48, 327–333.
Davies, K.J., Doroshow, J.H., 1986. Redox cycling of anthracyclines by cardiac mitochondria. I. Anthracycline radical formation by NADH dehydrogenase. J. Biol. Chem. 261, 3060–3067.
Ferrero, M.E., Ferrero, E., Gaja, G., Bernelli-Zazzera, A., 1976. Adriamycin: energy metabolism and mitochondrial oxidations in the heart of treated rabbits. Biochem. Pharmacol. 25, 125–130.
Gellerich, F.N., Kunz, W.S., Bohnensack, R., 1990. Estimation of flux control coefficients from inhibitor titrations by non-linear regression. FEBS Lett. 274, 167–170.
Gomez, L.A., Monette, J.S., Chavez, J.D., Maier, C.S., Hagen, T.M., 2009. Supercomplexes of the mitochondrial electron transport chain decline in the aging rat heart. Arch. Biochem. Biophys. 490, 30–35.
Gornall, A.G., Bardawill, C.J., David, M.M., 1949. Determination of serum proteins by means of the biuret reaction. J. Biol. Chem. 177, 751–766.

Groen, A.K., Wanders, R.J., Westerhoff, H.V., van der Meer, R., Tager, J.M., 1982. Quantification of the contribution of various steps to the control of mitochondrial respiration. J. Biol. Chem. 257, 2754–2757.

Hequet, O., Le, Q.H., Moullet, I., Pauli, E., Salles, G., Espinouse, D., Dumontet, C., Thieblemont, C., Arnaud, P., Antal, D., Bouafia, F., Coiffier, B., 2004. Subclinical late cardiomyopathy after doxorubicin therapy for lymphoma in adults. J. Clin. Oncol. Off. J. Am. Soc. Clin. Oncol. 22, 1864–1871.

Iwamoto, Y., Hansen, I.L., Porter, T.H., Folkers, K., 1974. Inhibition of coenzyme Q10-enzymes, succinoxidase and NADH-oxidase, by adriamycin and other quinones having antitumor activity. Biochem. Biophys. Res. Commun. 58, 633–638.

Kroemer, G., Galluzzi, L., Brenner, C., 2007. Mitochondrial membrane permeabilization in cell death. Physiol. Rev. 87, 99–163.

Long, J., Ma, J., Luo, C., Mo, X., Sun, L., Zang, W., Liu, J., 2009. Comparison of two methods for assaying complex I activity in mitochondria isolated from rat liver, brain and heart. Life Sci. 85, 276–280.

Luo, C., Long, J., Liu, J., 2008. An improved spectrophotometric method for a more specific and accurate assay of mitochondrial complex III activity. Clin. Chim. Acta 395, 38–41.

Machado, N.G., Baldeiras, I., Pereira, G.C., Pereira, S.P., Oliveira, P.J., 2010. Sub-chronic administration of doxorubicin to Wistar rats results in oxidative stress and unaltered apoptotic signaling in the lung. Chem. Biol. Interact. 188, 478–486.

Mazat, J.P., Letellier, T., Bedes, F., Malgat, M., Korzeniewski, B., Jouaville, L.S., Morkuniene, R., 1997. Metabolic control analysis and threshold effect in oxidative phosphorylation: implications for mitochondrial pathologies. Mol. Cell. Biochem. 174, 143–148.

Montaigne, D., Marechal, X., Preau, S., Baccouch, R., Modine, T., Fayad, G., Lancel, S., Neviere, R., 2011. Doxorubicin induces mitochondrial permeability transition and contractile dysfunction in the human myocardium. Mitochondrion 11, 22–26.

Moreno-Sanchez, R., Saavedra, E., Rodriguez-Enriquez, S., Olin-Sandoval, V., 2008. Metabolic control analysis: a tool for designing strategies to manipulate metabolic pathways. J. Biomed. Biotechnol. 2008, 597913.

Moulin, M., Piquereau, J., Mateo, P., Fortin, D., Rucker-Martin, C., Gressette, M., Lefebvre, F., Gresikova, M., Solgadi, A., Veksler, V., Garnier, A., Ventura-Clapier, R., 2015. Sexual dimorphism of doxorubicin-mediated cardiotoxicity: potential role of energy metabolism remodeling. Circ. Heart Fail. 8, 98–108.

Nicolay, K., de Kruijff, B., 1987. Effects of adriamycin on respiratory chain activities in mitochondria from rat liver, rat heart and bovine heart. Evidence for a preferential inhibition of complex III and IV. Biochim. Biophys. Acta 892, 320–330.

Oliveira, P.J., Wallace, K.B., 2006. Depletion of adenine nucleotide translocator protein in heart mitochondria from doxorubicin-treated rats–relevance for mitochondrial dysfunction. Toxicology 220, 160–168.

Ott, M., Robertson, J.D., Gogvadze, V., Zhivotovsky, B., Orrenius, S., 2002. Cytochrome c release from mitochondria proceeds by a two-step process. Proc. Natl. Acad. Sci. U. S. A. 99, 1259–1263.

Parker, M.A., King, V., Howard, K.P., 2001. Nuclear magnetic resonance study of doxorubicin binding to cardiolipin containing magnetically oriented phospholipid bilayers. Biochim. Biophys. Acta 1514, 206–216.

Pasdois, P., Parker, J.E., Halestrap, A.P., 2013. Extent of mitochondrial hexokinase II dissociation during ischemia correlates with mitochondrial cytochrome c release, reactive oxygen species production, and infarct size on reperfusion. J. Am. Heart Assoc. 2, e005645.

Pereira, G.C., Pereira, S.P., Pereira, C.V., Lumini, J.A., Magalhaes, J., Ascensao, A., Santos, M.S., Moreno, A.J., Oliveira, P.J., 2012. Mitochondrionopathy phenotype in doxorubicin-treated Wistar rats depends on treatment protocol and is cardiac-specific. PLoS One 7, e38867.

Rossignol, R., Malgat, M., Mazat, J.P., Letellier, T., 1999. Threshold effect and tissue specificity. Implication for mitochondrial cytopathies. J. Biol. Chem. 274, 33426–33432.

Rossignol, R., Letellier, T., Malgat, M., Rocher, C., Mazat, J.P., 2000. Tissue variation in the control of oxidative phosphorylation: implication for mitochondrial diseases. Biochem. J. 347 (Pt 1), 45–53.

Santos, D.L., Moreno, A.J., Leino, R.L., Froberg, M.K., Wallace, K.B., 2002. Carvedilol protects against doxorubicin-induced mitochondrial cardiomyopathy. Toxicol. Appl. Pharmacol. 185, 218–227.

Singal, P.K., Iliskovic, N., 1998. Doxorubicin-induced cardiomyopathy. N. Engl. J. Med. 339, 900–905.

Solem, L.E., Henry, T.R., Wallace, K.B., 1994. Disruption of mitochondrial calcium homeostasis following chronic doxorubicin administration. Toxicol. Appl. Pharmacol. 129, 214–222.

Solem, L.E., Heller, L.J., Wallace, K.B., 1996. Dose-dependent increase in sensitivity to calcium-induced mitochondrial dysfunction and cardiomyocyte cell injury by doxorubicin. J. Mol. Cell. Cardiol. 28, 1023–1032.

Spinazzi, M., Casarin, A., Pertegato, V., Ermani, M., Salviati, L., Angelini, C., 2011. Optimization of respiratory chain enzymatic assays in muscle for the diagnosis of mitochondrial disorders. Mitochondrion 11, 893–904.

Von Hoff, D.D., Layard, M.W., Basa, P., Davis Jr., H.L., Von Hoff, A.L., Rozencweig, M., Muggia, F.M., 1979. Risk factors for doxorubicin-induced congestive heart failure. Ann. Intern. Med. 91, 710–717.

Wallace, K.B., 2007. Adriamycin-induced interference with cardiac mitochondrial calcium homeostasis. Cardiovasc. Toxicol. 7, 101–107.

Yao, C.X., Li, W.Y., Zhang, S.F., Zhang, S.F., Zhang, H.F., Zang, M.X., 2011. Effects of doxorubicin and Fenofibrate on the activities of NADH oxidase and citrate synthase in mice. Basic Clin. Pharmacol. Toxicol. 109, 452–456.

Young, R.C., Ozols, R.F., Myers, C.E., 1981. The anthracycline antineoplastic drugs. N. Engl. J. Med. 305, 139–153.

Zhou, S., Starkov, A., Froberg, M.K., Leino, R.L., Wallace, K.B., 2001. Cumulative and irreversible cardiac mitochondrial dysfunction induced by doxorubicin. Cancer Res. 61, 771–777.